THE JOURNAL OF PHYSICAL CHEMISTRY C

Article

pubs.acs.org/JPCC

Insights into the Anomalous Vibrational Frequency Shifts of CO_2 Adsorbed to Metal Sites in Microporous Frameworks

Stephen A. FitzGerald,*[,†] Jennifer M. Schloss,[†,∥] Christopher J. Pierce,[†] Benjamin Thompson,[†] Jesse L. C. Rowsell,[‡] Kuang Yu,[§,⊥] and J. R. Schmidt[§]

[†]Department of Physics and Astronomy and [‡]Department of Chemistry and Biochemistry, Oberlin College, Oberlin, Ohio 44074, United States

[§]Theoretical Chemistry Institute and Department of Chemistry, University of Wisconsin—Madison, Madison, Wisconsin 53706, United States

Supporting Information

ABSTRACT: Diffuse reflectance infrared (IR) spectroscopy was used to study the structure and dynamics of H_2 and CO_2 adsorbed within the isostructural metal−organic frameworks M_2**L** (M = Mg, Mn, Fe, Co, Zn; **L** = 2,5-dioxidobenzene-1,4-dicarboxylate) referred to as M-MOF-74 and CPO-27-M. Cluster models of the primary adsorption site were excised from periodic models that were optimized using plane-wave density functional theory at the Perdew−Burke−Ernzerhof (PBE) level. Models incorporating an adsorbed H_2 or CO_2 were optimized using dispersion-corrected density functional theory (DFT), and the anharmonic vibrational frequencies of the adsorbate were calculated using the discrete variable representation method. The calculated vibrational frequency shifts reveal the same trend among the M_2**L** materials as those observed experimentally and provide insight into the origins of these shifts. Our experimental spectra of adsorbed CO_2 confirm a unique blue shift of the ν_3 mode for molecules adsorbed in Mg_2**L**, while the frameworks assembled from transition metals induce a red shift. By shifting the focus to the CO_2 *local* vibrational modes, a deeper insight into the influence of "back bonding" (metal d-electron density donation into CO_2 π^* orbitals) is revealed; for Mg_2**L** there is a near-complete cancellation of the opposing local mode contributions to the observed frequency shift. Additional spectral features in the CO_2 ν_3 region are assigned to (1) the ν_3 mode of the $^{13}CO_2$ isotopologue, (2) a combination mode involving a ν_2 excitation, and (3) librational sidebands arising from center-of-mass motion of the adsorbed molecule on the surface. Interestingly, below 100 K we observe the appearance of a new band that is distinct from the primary ν_3 band observed at room temperature. This band is attributed to an alternate, localized orientation of CO_2 adsorbed to the metal site, which is supported by the DFT model.

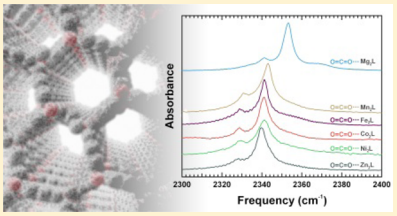

INTRODUCTION

Two gases have sustained the attention of environmental and energy science researchers in recent decades: H_2 and CO_2. From a chemistry standpoint, the former is an ideal energy carrier, being lightweight and producing only water during combustion or oxidative conversion in fuel cells. Dihydrogen is also the simplest molecular species, and its dynamics are the most amenable to accurate modeling by quantum theory. Yet no storage technology has been successfully commercialized to deliver practical quantities of the gas to an automobile motor.[1−3] In the case of CO_2, much attention has recently been focused on systems for efficient separation of CO_2 from gas mixtures, such as those at the heart of contemporary carbon capture and sequestration projects.[4−7] In both cases, microporous materials have been proposed as potential materials to overcome these gas storage and separation challenges, with their tremendous surface area yielding high gas uptake via physisorption.

Experimental benchmarks for modeling physisorptive interactions have traditionally been gathered using spectroscopy, wherein the perturbed energies of the translational, rotational, and vibrational quantum states of adsorbed molecules are measured. Infrared (IR) and inelastic neutron scattering (INS) spectroscopies are the primary techniques that have been employed to study H_2 and CO_2 adsorbed in microporous materials.[8−17] IR spectroscopy is especially useful because of the smaller capital cost and greater accessibility of the instrumentation, which is easily modified for in situ studies sampling a wide range of temperatures and pressures.[18] In all cases, the connections between spectroscopic observables and molecular structure and dynamics are indirect, often leaving results open to interpretation. Computational results provide an important bridge between experimental observables and the materials properties of interest. When computational results are inconsistent with experimental data, concerns about sample contamination or fundamental shortcomings in the underlying theory must be addressed. It is therefore essential to perform fundamental studies of robust, structurally simple adsorbents using complementary methods to confidently describe adsorption processes for even the smallest of molecules.

Crystalline metal−organic frameworks (MOFs) are ideal materials for fundamental gas adsorption studies. An exemplary

Received: October 16, 2014
Revised: February 20, 2015
Published: February 20, 2015

DOI: 10.1021/jp5104356
J. Phys. Chem. C 2015, 119, 5293−5300

group of such materials is the isostructural series variously referred to as M-MOF-74 or CPO-27-M.[19−21] This hexagonal structure type is assembled from M^{II} cations bridged by 2,5-dioxidobenzene-1,4-dicarboxylate, and will be referred to herein as M_2**L** for brevity. When completely desolvated, the channels of these materials are lined with metals having available coordination sites. This structural attribute has been associated with greater gas uptake under small partial pressure.[22−24] Independent analyses have demonstrated that the Ni_2**L** compound exhibits one of the largest (in magnitude) isosteric enthalpies of H_2 adsorption, approaching −13 kJ/mol at small surface coverage.[23−26] Using IR spectroscopy, several of these authors confirmed a distinct correlation between the red shift of the fundamental vibrational mode of H_2 and its enthalpy of adsorption at the metal sites.[27] This observation is consistent with the traditional view of the interaction between H_2 and metals, involving both $H_2(\sigma) \rightarrow M(nd)$ charge transfer and $M(nd) \rightarrow H_2(\sigma^*)$ "back bonding".[28]

Despite numerous experimental and computational studies of CO_2 adsorbed in the M_2**L** series, a detailed picture of the structure and dynamics of this seemingly uncomplicated adsorbate molecule is still emerging. In contrast to H_2, it is the Mg_2**L** compound that has the largest affinity for CO_2, with experimental isosteric enthalpies of adsorption reported to be around −45 kJ/mol.[29−34] IR spectroscopy has been employed to examine the asymmetric mode (ν_3) of CO_2 adsorbed by a few members of the M_2**L** series, with independent groups reporting small frequency shifts having no clear correlation with other properties of the materials.[16,17,35,36] There is also a curious difference in the direction of the frequency shifts: Mg_2**L** induces a blue shift of the ν_3 mode, while the transition metal analogues cause a red shift. The literature contains a variety of explanations for this behavior and a range of discrepant values predicted for the Mg_2**L**-induced frequency shift.[16,36,37] X-ray and neutron diffraction studies of Ni_2**L** and Mg_2**L** have provided compelling evidence for preferential adsorption of CO_2 to the available metal coordination sites, in a similar manner as H_2.[34,35,38,39] To gain further insight about the localized interaction of CO_2 with the Mg sites, ^{13}C nuclear magnetic resonance (NMR) spectroscopy was recently used to study the rotational motion of the adsorbate.[40] A reinterpretation of the thermal evolution of the spectra was later presented, and was supported by Monte Carlo simulations of the adsorbed CO_2.[41]

This report describes our collaborative effort to correctly assign the infrared spectroscopic features of H_2 and CO_2 adsorbed in the system of M_2**L** materials using insight provided by computational models. We find these models successfully calculate the same trends in vibrational frequency shifts observed in the experimental spectra, despite the contrasting behavior of the two adsorbate molecules. Importantly, we find that the seemingly anomalous spectroscopic signature of adsorbed CO_2 becomes straightforward when examined via a "local mode" perspective, thus providing clear physical insight into the nature of the metal−CO_2 interaction.

PROCEDURE

Samples of the microporous M_2**L** adsorbents were prepared and characterized as described in a previous publication.[27] After desolvation, all sample manipulations were performed under air-free conditions in an argon glovebox to prevent the adsorption of water or other coordinating species.

Infrared spectra were acquired using a Bomem DA3 Michelson interferometer equipped with quartz halogen and globar sources, a CaF_2 beamsplitter, and a liquid nitrogen cooled mercury cadmium telluride detector. A custom-built diffuse reflectance system with a sample chamber that allows both the temperature and atmosphere of the material to be controlled was utilized for all experiments.[18] Samples of M_2**L** (∼10 mg) were transferred under inert atmosphere to a sample cell affixed to a copper slab providing thermal contact to a cold-finger cryostat (Janis ST-300T). Prior to the introduction of CO_2 gas (purity >99.5%), samples were evacuated for several hours at room temperature (294 K). Dosing was achieved at room temperature by loading a calibrated volume to a desired pressure of CO_2, measured using an Omega PX-303 pressure transducer, and then exposing this gas to the sample cell. The pressure decrease was used to determine the adsorbed concentration of CO_2. Control runs were performed with He gas to evaluate dead-volume corrections. For spectra obtained below room temperature, no further gas was added to the system, but the pressure was monitored to determine if any additional adsorption occurred. The temperature was maintained with a Lake Shore 331 controller and monitored with a silicon diode thermometer mounted by the sample.

In silico models of the crystalline adsorbents were constructed using the reported atomic coordinates of the solvent-free framework determined by single-crystal X-ray diffraction,[20] and then optimized for each metal using plane-wave density functional theory at the Perdew−Burke−Ernzerhof (PBE) level with the Vienna Ab initio Simulation Package.[42−45] The calculations employed a 520 eV cutoff, with core electrons treated with the projector augmented wave (PAW) approach and structures converged to within 10 meV/Å. Finite cluster models containing three metals and bridging organic fragments were excised from each of the periodic models to higher-level treatments of the adsorbate−framework interactions. The size convergence of the cluster models was examined by comparing their results with periodic plane-wave calculations. At a lower yet consistent level of theory (PBE), the computed frequency shifts using both methods agree within 4% for H_2 and 1% for CO_2, validating the fidelity of our truncation method used in the cluster model. After inserting a H_2 or CO_2 at the primary adsorption site identified by diffraction studies,[35,46] geometry optimizations were conducted using density functional theory (DFT) incorporating Grimme's D2 dispersion correction.[47] In each case, the atomic positions of the adsorbate molecule, the central metal, and the five oxygens bonded to this metal were relaxed while the positions of the other atoms remained fixed. The maximum components of all forces were converged within 1 meV/Å. An Ahlrichs def2-TZVP basis set was used for the central metal atom and adsorbate molecule, while a smaller def2-SVP basis set was used for the other atoms. Following prior work,[24,48] and consistent with the spin states of similar coordination compounds having O-donor ligands, we adopted high-spin configurations for Mn, Fe, Co, and Ni. Additionally, we implemented ferromagnetic spin configurations where appropriate, since our previous work on the Cr^{3+}-containing framework MIL-101 indicated this configuration is slightly lower in energy.[49] The anharmonic vibrational frequencies were computed using the discrete variable representation (DVR) method. In all cases, we observed that the intramolecular potential energy surface (PES) of the adsorbate is best described by PBE0, prompting the use of a "hybrid" approach, as described below. Specifically,

DOI: 10.1021/jp5104356
J. Phys. Chem. C 2015, 119, 5293−5300

geometry optimization at the B3LYP-D (H_2) or PBE0-D (CO_2) level was followed by normal-mode analysis. The choice of B3LYP-D for H_2 was motivated by the functional's accurate reproduction of the M···H_2 bond distance as compared to higher-level wave function approaches (vide infra). Subsequent one-dimensional scans were performed along the computed normal mode coordinate at the PBE0-D level, at which point a DVR analysis was performed to compute the anharmonic frequency. This hybrid approach accounts for potential displacement of the B3LYP versus PBE0 minima along the normal mode coordinates, and fully accounts for the diagonal anharmonicity while neglecting any off-diagonal anharmonicity. Further details of the cluster models and additional validation data are provided in the Supporting Information.

RESULTS AND DISCUSSION

We began by benchmarking our computational methods with the diffuse reflectance IR spectra of H_2 adsorbed in six M_2**L** materials (M = Mg, Mn, Fe, Co, Ni, Zn). At low temperature and pressure the fundamental vibrational mode of para-H_2, denoted $Q(0)$, can be confidently assigned for molecules bound to the available metal coordination sites in each material.[27] A comparison of the experimentally measured frequency shifts of the H_2 $Q(0)$ mode with those calculated using our DFT approach is presented in Table 1. The same trend is noted in both cases. This trend parallels the Irving–Williams series, as was previously noted for the isosteric enthalpies of H_2 adsorption (at low surface coverage) for these materials.[24] The correlation between the spectroscopic and thermodynamic results is also shared by the M···H_2 interaction distances determined by neutron diffraction, as summarized in Table 1. Several authors have remarked about the consistency of these distinct experimental data with respect to the Kubas-type bonding mechanism used to describe gas adsorption at the metal sites.[13,23,27,50] Our computational models successfully reproduce these trends in frequency shifts and M···H_2 distances.

Table 1. Comparison of Experimental and Theoretical Quantities for H_2 Adsorbed at the Metal Site in M_2L Materials[a]

M	$\Delta\nu_{expt}$[b] (cm^{-1})	$\Delta\nu_{theo}$ (cm^{-1})	$d_{M\cdots H_2,expt}$ (Å)	$d_{M\cdots H_2,theo}$ (Å)
Mg	−69	−71	2.45[c]	2.41
Mn	−73	−83	n/a	2.62
Fe	−100	−96	2.47[d]	2.53
Co	−114	−104	n/a	2.51
Ni	−125	−139	2.20[e]	2.13
Zn	−65	−69	2.6[f]	2.57

[a]$\Delta\nu$ is the frequency shift of the fundamental vibration $Q(0)$, and $d_{M\cdots H_2}$ is the distance between the metal and the center of mass of the adsorbed H_2. [b]Data from refs 26 and 27. [c]Reference 52. [d]Reference 53. [e]Reference 54. [f]Reference 46.

Our calculated frequency shifts for H_2 are significantly larger than those calculated by Chabal and co-workers using van der Waals DFT,[51] likely due to the sensitivity of the shifts to the M···H_2 distances. Those distances are often poorly described by many pure generalized gradient approximation (GGA) functionals (and even some hybrid functionals), and our use of B3LYP-D was chosen after comparison with higher-level wave function-based calculations.

The vibrational structure of CO_2 is obviously more complex than that of H_2. There are three fundamental vibration modes to consider: the ν_1 symmetric stretch which is not IR active, the ν_2 bending mode which is doubly degenerate, and the ν_3 asymmetric stretching mode which is strongly IR active (only the P and R rovibrational branches are observed in the gas phase). Using the same techniques, instrumentation, and materials described in previous investigations of adsorbed H_2 isotopologues,[26,27] we measured the IR spectra of adsorbed CO_2 at various pressures and temperatures. For this report we focus on the ν_3 mode, as its frequency appears to be most sensitive to site-specific interactions. Figure 1 shows the IR absorption bands assigned to the ν_3 modes of CO_2 adsorbed at the metal site within the isostructural M_2**L** materials. Focusing on the most intense band, we confirm the Mg material is unique in displaying a blue shift relative to the gas phase frequency (dashed line in Figure 1), and our spectra are similar to previous reports on a subset of these materials.[16,17,35,36] The strong IR absorbance of CO_2 in Mg_2**L** at a relatively small equilibrium pressure is consistent with the significantly enhanced interaction of the molecule with this particular metal.

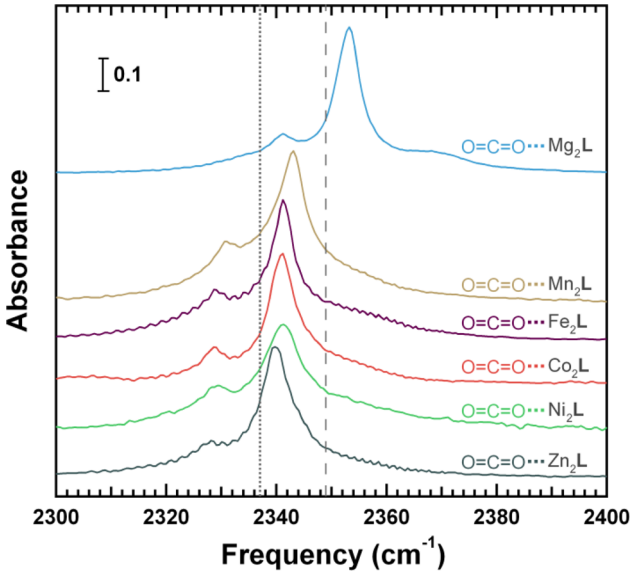

Figure 1. Diffuse reflectance IR spectra of adsorbed CO_2 in isostructural M_2**L** materials at 293 K. The dashed line at 2349 cm^{-1} marks the gas phase CO_2 ν_3 frequency and the dotted line at 2337 cm^{-1} marks the much weaker band involving the ν_3 transition of CO_2 in the first excited ν_2 level. Equilibrium pressures measured during acquisition of the spectra (top to bottom) were 0.2, 1.4, 6.4, 1.8, 6.2, and 11 mbar, respectively. All pressures correspond to concentrations of less than 0.02 CO_2 per M. Spectra were measured with 1 cm^{-1} resolution and are offset for clarity.

Working toward an understanding of the origin of the unique IR signature of CO_2 in Mg_2**L**, we computed the $\Delta\nu_3$ frequency shifts using the methods described above for H_2 adsorption. The results of the DVR calculations are listed in Table 2 alongside the experimental values gleaned from Figure 1. Although the frequency shifts are small, the theory correctly predicts the observed trend. The anomalous blue shift observed for Mg_2**L** was previously ascribed to asymmetric distortion of the CO_2 molecule upon adsorption,[16] yet our calculations show no obvious differences in binding geometry or orientation among the optimized structures. Unlike H_2, there is little

DOI: 10.1021/jp5104356
J. Phys. Chem. C 2015, 119, 5293−5300

Table 2. Comparison of Experimental and Theoretical Quantities for CO_2 Adsorbed at the Metal Site in M_2L Materials[a]

M	$\Delta\nu_{3,expt}$ (cm^{-1})	$\Delta\nu_{3,theo}$ (cm^{-1})	$\Delta\omega_{1,theo}$ (cm^{-1})	$\Delta\omega_{2,theo}$ (cm^{-1})	$d_{M\cdots OCO,expt}$ (Å)	$d_{M\cdots OCO,theo}$ (Å)	ΔH_{expt} (kJ/mol)	E_{theo} (kJ/mol)
Mg	4	2	−53	53	2.24−2.39,[b] 2.27[c]	2.27	−43.5,[c] −47,[e] −42,[f] −39,[g] −73,[h], −45,[i] −42.0[j]	−44
Mn	−6	−5	−45	35	2.51[c]	2.51	−31.7,[c] −31.9[j]	−33
Fe	−8	−5	−43	34	2.29[c]	2.46	−33.2,[c] −34.3[j]	−32
Co	−8	−6	−48	38	2.23,[c] 2.261[c]	2.38	−33.6,[c] −37,[e] −34.5[j]	−34
Ni	−8	−6	−56	44	2.29[d]	2.29	−38.6,[c] −40,[d], −41,[e] −39,[f] −38.7[j]	−39
Zn	−9	−6	−46	35	2.43[c]	2.44	−26.8,[c] −30,[i] −30.6[j]	−33

[a] $\Delta\nu_3$ is the frequency shift of the asymmetric stretching (normal) mode, $\Delta\omega_1$ is the frequency shift of the local vibrational mode of the C−O bond nearest the metal, $\Delta\omega_2$ is the frequency shift of the local vibrational mode of the C−O bond farthest from the metal, $d_{M\cdots OCO}$ is the distance between the metal and the nearest oxygen atom of the adsorbed CO_2, ΔH_{expt} is the enthalpy of adsorption (at small surface coverage) determined by isosteric analysis of gas adsorption isotherms or variable-temperature IR spectroscopy, and E_{theo} is the calculated energy of adsorption. [b] Data from ref 39. [c] Reference 34. [d] Reference 35. [e] Reference 29. [f] Reference 30. [g] Reference 31. [h] Reference 55. [i] Reference 32. [j] Reference 33.

correlation of the CO_2 frequency shifts with the M···adsorbate distances or adsorption enthalpies, but the optimized structures match the experimental geometries quite well, with the exception of M = Fe (see Table 2). Our calculated geometries do not display the bending distortions of CO_2 that were originally reported from diffraction models,[35,38,39] in agreement with a more recent study that concluded these distortions to be artifacts of the CO_2 orientation disorder.[34]

A more transparent explanation for the IR signature of CO_2 in these model compounds arises when the vibrations are examined from a local mode perspective. In this view, the focus is on the individual C−O bond vibrations, which give rise to the symmetric and asymmetric normal modes through strong vibrational coupling. The normal mode and local mode coordinates are two equivalent basis sets to construct the molecular vibrational Hamiltonian, and the transformation between these two basis sets can be performed using the **FG** decomposition formalism (see, for example, ref 56). Within this formalism, we decomposed the symmetric and asymmetric normal modes of our computed models into two local C−O stretching modes (i.e., bond vibrations), within the harmonic approximation, yielding a vibrational Hamiltonian in a local mode basis. The calculated harmonic frequencies are essentially identical to their anharmonic counterparts calculated via DVR as described above, validating this additional approximation. As might be expected, the coupling is large (~450 cm^{-1}) but essentially constant among the six materials. This coupling gives rise to the usual symmetric and asymmetric normal modes (of which the latter is the experimental observable in this case). Here we focus on the constituent local modes (C−O bond vibrations), which demonstrate more significant frequency shifts and serve as more direct probes of the metal−CO_2 interaction. As shown in Table 2, the local mode of the C2−O1 bond, which is closer to the metal atom, exhibits a strong red shift in all cases ($\Delta\omega_1$), while the local mode of C2−O3 is blue-shifted ($\Delta\omega_2$). This is consistent with the interaction of the CO_2 quadrupole moment with the electric field of a point charge. Polarization and charge transfer may further weaken the C2−O1 bond due to its proximity to the metal center. As mentioned above, the coupling between the two CO_2 local modes is approximately the same in all of the materials. As such, the small frequency shift of the ν_3 asymmetric stretch can be interpreted as arising from the opposition between the red- and blue-shifted local modes, which yield only small residual frequency shifts when these modes couple to form the resulting normal modes (given by the eigenvalue of the vibrational Hamiltonian). In contrast to the transition-metal-containing materials, these two shifts are comparable in size for CO_2 in Mg_2L. We attribute this behavior to an absence of d valence electrons at the Mg site, which precludes "back bonding" (electron density donation into CO_2 π^* orbitals). Such an interaction is expected to additionally red shift both local modes approximately equally, yielding a net red shift of the asymmetric stretch.

The conclusions drawn from the local mode analysis are supported by natural bond orbital (NBO) calculations. An isolated gas-phase CO_2 can be described as a resonance hybrid, with double−double, single−triple, and triple−single bond character within the three dominant Lewis structures. In contrast, NBO analysis[57] of the adsorbed CO_2 shows that the single (C2−O1)−triple (C2−O3) resonance structure dominates, likely due to polarization effects. This deviation matches the trends of the computed local frequency shifts, with a red shift of the C2−O1 local mode and a blue shift of the C2−O3 mode. The exception is CO_2 in Fe_2L, which displays dominant double−double bonding configuration, consistent with its smaller CO_2 local mode shifts. Among the other metals, the magnitudes of the blue C2−O3 frequency shifts are anticorrelated with the non-Lewis antibonding ($\pi^* + \sigma^*$) occupancies of the C2−O3 bonds (see Supporting Information, Figure S1), consistent with the idea that the local mode frequency shifts are directly related to interactions which modulate the bonding character of the C−O bonds. The C2−O3 bond in the Mg_2L case has the smallest antibonding occupancy (due to the missing back-bonding interaction) and thus the largest local blue shift.

Overall, this theoretical approach provides good agreement with the experimental $\Delta\nu_3$ values shown in Table 2. The model correctly predicts a unique blue shift for CO_2 in Mg_2L and red shifts when this molecule interacts with transition metal sites. All of the calculated frequency shifts are within a few wavenumbers of the experimental results. For comparison, previous theoretical calculations have shown a large range in values for $\Delta\nu_3$ (10−15 cm^{-1} blue,[36] 6−17 cm^{-1} blue,[37] 0.5 cm^{-1} red[16]).

The insight provided by the local mode analysis for CO_2 can be extended to correlations among other observable properties. In contrast with the asymmetric mode frequency shifts, the local mode frequency shifts correlate well with the experimental enthalpies of adsorption and calculated adsorption energies for the transition-metal-containing materials. Again, the unique nature of Mg_2L is highlighted by this comparison. Recent theoretical studies have suggested that one can understand the trends in adsorption energy in terms of a combination of

DOI: 10.1021/jp5104356
J. Phys. Chem. C 2015, 119, 5293−5300

electrostatic effects (which are maximized for Mg) and crystal-field-type arguments.[33,58,59] In the case of simple diatomic adsorbates (such as H_2), the local and normal mode pictures are equivalent, and the normal mode (and thus direct spectroscopic observable) trivially correlates with adsorption energies. When dealing with complex polyatomic molecules, however, the local mode perspective may yield a more intuitive explanation of the metal−adsorbate interactions.

We have also assigned the weaker bands in the IR spectra shown in Figure 1. At the low CO_2 concentrations examined, all of the spectra exhibit a much less intense shoulder red-shifted 12 cm^{-1} from the primary band. Data for gas phase CO_2 vibrational transitions from the HITRAN database indicate that this shoulder is a combination band in which a molecule in the first excited bending mode (ν_2) undergoes a fundamental transition of the asymmetric stretching mode (ν_3).[60] The fact that this shoulder is red-shifted from the primary band by the same frequency for all samples is more consistent with its assignment as a combination mode and not the pure ν_3 transition of a CO_2 adsorbed on a different site, especially at these small pressures. Other workers have attributed this shoulder to a combination transition of the ν_3 asymmetric stretching mode and the two ν_2 bending modes whose degeneracy is broken upon adsorption.[16] We conclude that there is no need to invoke a lifting of the ν_2 degeneracy, as the shoulder has the same shift from the pure ν_3 transition as observed for gas phase CO_2.

A closer inspection of the CO_2 IR spectra reveals the presence of broad sidebands in addition to the sharper features. A spectrum acquired with the Mg material was deconvoluted into five Lorentzian curves (see Figure 2, where a wider frequency range is shown). The three sharp bands are assigned to ν_3-based transitions, all blue shifted by comparable amounts from the gas phase frequencies listed in the HITRAN database. In order of decreasing frequency they are the fundamental ν_3 (2353 cm^{-1}), the combination band with ν_2 (2341 cm^{-1}), and the fundamental ν_3 band of the $^{13}CO_2$ isotopologue (2286 cm^{-1}). The fundamental bands of the isotopologues are both shifted from gas phase frequencies by the same 2.8 cm^{-1}, while the combination band is shifted by 3.6 cm^{-1}. The intensity ratio between the fundamental band and the combination band differs from the ratio listed in HITRAN by a factor of 0.84, which stems from the tendency of the diffuse reflectance method to enhance low-intensity features. The two broader sidebands appear symmetrically shifted by 15.3 cm^{-1} to each side of the fundamental band. They were also fit with Lorentzian curves, constrained such that their areas are related by the Boltzmann factor for population of two energy states differing by 15.3 cm^{-1}. It is probable that these sidebands correspond to translational or librational transitions occurring with the ν_3 fundamental transition. This interpretation is consistent with structural models from neutron diffraction studies[38] and recent NMR studies which suggest orientational fluctuations of the bound CO_2 about its minimum-energy configuration.[41]

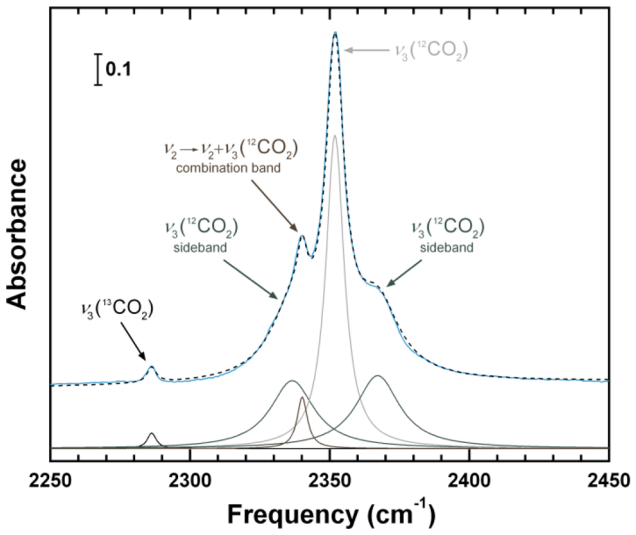

Figure 2. Curve fitting of a spectrum of adsorbed CO_2 in Mg_2**L** at 293 K with an equilibrium pressure of 20 mbar, corresponding to a concentration of 0.1 CO_2 per Mg. The solid blue trace is the observed spectrum, and the dotted black trace is the summative fit. Gray traces are the five Lorentzian functions comprising the fit, which have been vertically offset for clarity.

Additional observations related to the dynamics of bound CO_2 are provided by IR spectra collected at lower temperatures. The thermal evolution of spectra acquired from CO_2 adsorbed by Mg_2**L** is shown in Figure 3. The gas loading conditions were chosen such that, at room temperature, greater than 95% of the CO_2 molecules in the system are in the adsorbed phase. Since the system is sealed during cooling, we can take the adsorbed concentration to be essentially constant, with at most a 5% increase at the lowest temperature. First, it can be noted that the combination band (2341 cm^{-1}) disappears upon cooling, as expected for a band originating from CO_2 in an excited (ν_2) vibrational state. Consistent with the findings of Valenzano et al.,[36] we do not observe any shift (within 0.1 cm^{-1}) in the frequency of the adsorbed species upon cooling to 100 K. This is not surprising, given the very small lattice constant change of Mg_2**L** in this temperature range.[39] More striking is the appearance at 75 K of a new band at 2355 cm^{-1} that is distinguishable from the fundamental ν_3 (2353 cm^{-1}). The higher frequency band continues to increase in intensity with decreasing temperature at the expense of the other. The two bands also sharpen with cooling, allowing a deconvolution of the spectra into two Lorentzian line shapes. Based on the relative area of these bands, we use a van't Hoff plot (see Supporting Information, Figure S2) to estimate that the enthalpy difference between their configurations is ∼1 kJ/mol. While the lower enthalpy configuration (associated with the 2355 cm^{-1} band) is favored at low temperature, the higher enthalpy configuration (associated with the 2353 cm^{-1} band) is dominant at higher temperature. Thus, a simple Gibbs free energy consideration, $\Delta G = \Delta H - T\Delta S$, shows that this higher enthalpy configuration also has a higher entropy, which our van't Hoff plot puts at ∼6 J K^{-1} mol^{-1}. We hypothesize that each band corresponds to a unique molecular orientation at the primary binding site of the Mg atom. Previous theoretical treatments[61] examining the rotations of an adsorbed CO_2 about a metal center (crudely corresponding to transitions between the two orientations) estimate the energy barrier to be less than 3 kJ/mol, which would allow for interconversion even below 100 K, and thus we can assume the populations of these states are in equilibrium without considering the detailed kinetics of their interconversion. An alternate interpretation of the second band as arising from the occupancy of a secondary site is discounted by a recent NMR study that showed hopping of the CO_2 between different adsorption sites is frozen out below 150 K.[41]

DOI: 10.1021/jp5104356
J. Phys. Chem. C 2015, 119, 5293−5300

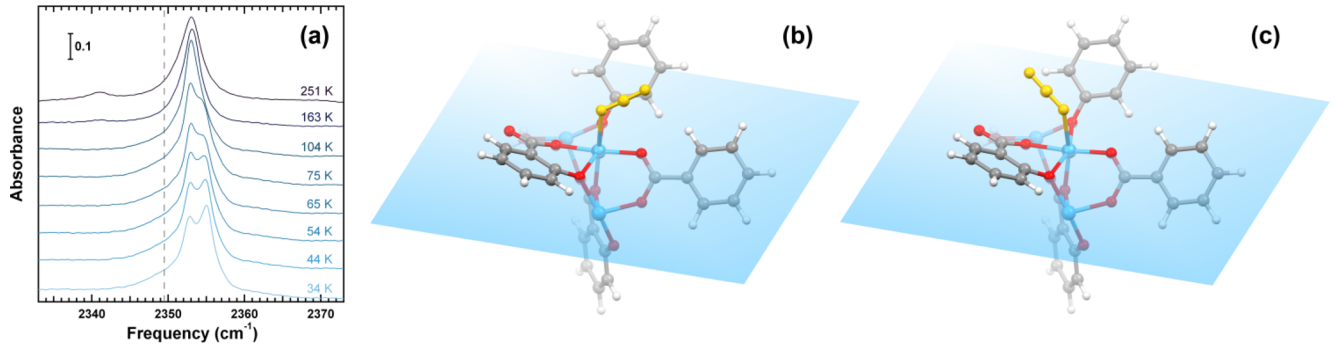

Figure 3. (a) Temperature dependence of the IR spectra of adsorbed CO_2 in Mg_2**L** at a concentration of 0.025 CO_2 per Mg. The dashed line at 2349 cm^{-1} represents the gas phase ν_3 frequency. (b) Minimum energy orientation of CO_2 (yellow) bound to the adsorption site of a trimetallic cluster model calculated by hybrid DFT methods. (c) Alternate orientation for CO_2 in a local minimum of the same adsorption site. Framework atom colors: C, gray; H, white; Mg, blue; O, red. The blue rectangles represent the mean planes defined by Mg and the four equatorial O atoms in its coordination sphere.

Our DFT calculations confirm the existence of two stable CO_2 adsorption configurations at the primary binding site (see Figure 3). Both involve close approach of a CO_2 oxygen atom with the Mg atom (2.27 Å vs 2.28 Å). The lower energy configuration is more strongly bound due to the shorter distance between the CO_2 carbon and a carboxyl oxygen of the framework (2.75 Å vs 3.07 Å). As such, we predict that the more energetically stable configuration is also lower in entropy, and is thus relatively disfavored at higher temperatures, consistent with dominance of the 2353 cm^{-1} band. A harmonic vibrational analysis predicts a larger blue shift for this secondary configuration (5.5 cm^{-1} vs 2 cm^{-1}), consistent with the experimentally observed frequency difference between the two bands (Figure 3). It should be noted, however, that the calculated energy difference between the two configurations is 8 kJ/mol, larger than the experimental estimate. This may be due to the simplicity of the van't Hoff analysis which assumes that both entropy and enthalpy changes are constant below 100 K. In particular, the large residual conformational freedom of the adsorbed CO_2 may generate a nontrivial temperature dependence of the entropy difference between the two configurations.

CONCLUSIONS

Diffuse reflectance IR spectroscopy provides a detailed probe of the adsorbate−metal interactions in microporous MOFs with coordinatively unsaturated metal sites. We interpret the spectroscopic frequency shifts in terms of perturbations arising from a combination of electrostatics and charge transfer, unique to each metal and adsorbate molecule involved. For polyatomic molecules, the coupling of the adsorbate local modes into normal modes can mask these simple trends, but we find that an intuitive interpretation is restored through a straightforward local mode transformation. For the case of CO_2 in Mg_2**L**, our results explain the seemingly anomalous blue shift of the asymmetric ν_3 mode in terms of the small difference between large and opposing frequency shifts in the two local C−O modes. The size of these calculated local mode shifts is seen to correlate with the binding energy of CO_2 at the metal site. The occurrence of broad sidebands symmetrically shifted from the ν_3 mode is assigned to librational behavior associated with the rotational degree of freedom of the bound CO_2. This orientational freedom is also interpreted as the origin of the two low temperature bands, associated with distinct local-minimum-energy configurations.

ASSOCIATED CONTENT

Supporting Information

Correlation plot from natural bond order analysis, van't Hoff analysis plots, supplementary diagrams of the calculated CO_2 orientations at the primary adsorption site, fractional atomic coordinates and unit cell information for calculated periodic models, atomic coordinates of DFT cluster models. This material is available free of charge via the Internet at http://pubs.acs.org.

AUTHOR INFORMATION

Corresponding Author

*E-mail: stephen.fitzgerald@oberlin.edu. Tel.: (440) 775-8334.

Present Addresses

[‖]MIT−Harvard Center for Ultracold Atoms, Research Laboratory of Electronics, and Department of Physics, Massachusetts Institute of Technology, Cambridge, MA 02139, USA.

[⊥]Department of Mechanical and Aerospace Engineering, Princeton University, Princeton, NJ 08533-5263, USA.

Notes

The authors declare no competing financial interest.

ACKNOWLEDGMENTS

This work was partially supported by the National Science Foundation (Award No. CHE-1111896) and the U.S. Department of Energy (Award No. DE-FG02-09ER16059). J.R.S. is an Alfred P. Sloan Research Fellow and a Camille Dreyfus Teacher−Scholar. We are saddened to report the untimely death of Jesse Rowsell during the final editing of the manuscript.

REFERENCES

(1) Schlapbach, L.; Züttel, A. Hydrogen-storage materials for mobile applications. *Nature* **2001**, *414*, 353−358.

(2) Yang, J.; Sudik, A.; Wolverton, C.; Siegel, D. J. High capacity hydrogen storage materials: attributes for automotive applications and techniques for materials discovery. *Chem. Soc. Rev.* **2010**, *39*, 656−675.

(3) Schlichtenmayer, M.; Hirscher, M. Nanosponges for hydrogen storage. *J. Mater. Chem.* **2012**, *22*, 10134−10143.

(4) Haszeldine, R. S. Carbon capture and storage: how green can black be? *Science* **2009**, *325*, 1647−1652.

(5) Keskin, S.; van Heest, T. M.; Sholl, D. S. Can metal−organic framework materials play a useful role in large-scale carbon dioxide separations? *ChemSusChem* **2010**, *3*, 879−891.

DOI: 10.1021/jp5104356
J. Phys. Chem. C 2015, 119, 5293−5300

(6) Sumida, K.; Rogow, D. L.; Mason, J. A.; McDonald, T. M.; Bloch, E. D.; Herm, Z. R.; Bae, T.-H.; Long, J. R. Carbon dioxide capture in metal-organic frameworks. *Chem. Rev.* **2012**, *112*, 724−781.
(7) Hedin, N.; Andersson, L.; Bergström, L.; Yan, J. Adsorbents for the post-combustion capture of CO_2 using rapid temperature swing or vacuum swing adsorption. *Appl. Energy* **2013**, *104*, 418−433.
(8) Nicol, J. M.; Eckert, J.; Howard, J. Dynamics of molecular hydrogen adsorbed in CoNa-A zeolite. *J. Phys. Chem.* **1988**, *92*, 7117−7121.
(9) Forster, P. M.; Eckert, J.; Chang, J.-S.; Park, S. E.; Férey, G.; Cheetham, A. K. Hydrogen adsorption in nanoporous nickel(II) phosphates. *J. Am. Chem. Soc.* **2003**, *125*, 1309−1312.
(10) Rowsell, J. L. C.; Eckert, J.; Yaghi, O. M. Characterization of H_2 binding sites in prototypical metal-organic frameworks by inelastic neutron scattering. *J. Am. Chem. Soc.* **2005**, *127*, 14904−14910.
(11) Ramirez-Cuesta, A. J.; Jones, M. J.; David, W. I. F. Neutron scattering and hydrogen storage. *Mater. Today* **2009**, *12*, 54−61.
(12) Matanović, I.; Belof, J. L.; Space, B.; Sillar, K.; Sauer, J.; Eckert, J.; Bačić, Z. Hydrogen adsorbed in a metal organic framework-5: coupled translation-rotation eigenstates from quantum five-dimensional calculations. *J. Chem. Phys.* **2012**, *137*, 014701.
(13) Bordiga, S.; Vitillo, J. G.; Ricchiardi, G.; Regli, L.; Cocina, D.; Zecchina, A.; Arstad, B.; Bjorgen, M.; Hafizovic, J.; Lillerud, K. P. Interaction of hydrogen with MOF-5. *J. Phys. Chem. B* **2005**, *109*, 18237−18242.
(14) FitzGerald, S. A.; Allen, K.; Landerman, P.; Hopkins, J.; Matters, J.; Myers, R.; Rowsell, J. L. C. Quantum dynamics of adsorbed H_2 in the microporous framework MOF-5 analyzed using diffuse reflectance infrared spectroscopy. *Phys. Rev. B* **2008**, *77*, 224301.
(15) Kong, L. Z.; Chabal, Y. J.; Langreth, D. C. First-principles approach to rotational-vibrational frequencies and infrared intensity for H_2 adsorbed in nanoporous materials. *Phys. Rev. B* **2011**, *83*, 121402.
(16) Yao, Y. P.; Nijem, N.; Li, J.; Chabal, Y. J.; Langreth, D. C.; Thonhauser, T. Analyzing the frequency shift of physiadsorbed CO_2 in metal organic framework materials. *Phys. Rev. B* **2012**, *85*, 064302.
(17) Nijem, N.; Canepa, P.; Kong, L. Z.; Wu, H. H.; Li, J.; Thonhauser, T.; Chabal, Y. J. Spectroscopic characterization of van der Waals interactions in a metal organic framework with unsaturated metal centers: MOF-74-Mg. *J. Phys.: Condens. Matter* **2012**, *24*, 424203.
(18) FitzGerald, S. A.; Churchill, H. O. H.; Korngut, P. M.; Simmons, C. B.; Strangas, Y. E. Cryogenic apparatus for diffuse reflection infrared spectroscopy with high-pressure capabilities. *Rev. Sci. Instrum.* **2006**, *77*, 093110.
(19) Rosi, N. L.; Kim, J.; Eddaoudi, M.; Chen, B. L.; O'Keeffe, M.; Yaghi, O. M. Rod packings and metal-organic frameworks constructed from rod-shaped secondary building units. *J. Am. Chem. Soc.* **2005**, *127*, 1504−1518.
(20) Dietzel, P. D. C.; Morita, Y.; Blom, R.; Fjellvåg, H. An in situ high-temperature single-crystal investigation of a dehydrated metal−organic framework compound and field-induced magnetization of one-dimensional metal−oxygen chains. *Angew. Chem., Int. Ed.* **2005**, *44*, 6354−6358.
(21) Dietzel, P. D. C.; Johnsen, R. E.; Blom, R.; Fjellvåg, H. Structural changes and coordinatively unsaturated metal atoms on dehydration of honeycomb analogous microporous metal−organic frameworks. *Chem.—Eur. J.* **2008**, *14*, 2389−2397.
(22) Rowsell, J. L. C.; Yaghi, O. M. Effects of functionalization, catenation, and variation of the metal oxide and organic linking units on the low-pressure hydrogen adsorption properties of metal-organic frameworks. *J. Am. Chem. Soc.* **2006**, *128*, 1304−1315.
(23) Vitillo, J. G.; Regli, L.; Chavan, S.; Ricchiardi, G.; Spoto, G.; Dietzel, P. D. C.; Bordiga, S.; Zecchina, A. Role of exposed metal sites in hydrogen storage in MOFs. *J. Am. Chem. Soc.* **2008**, *130*, 8386−8396.
(24) Zhou, W.; Wu, H.; Yildirim, T. Enhanced H_2 adsorption in isostructural metal-organic frameworks with open metal sites: strong dependence of the binding strength on metal ions. *J. Am. Chem. Soc.* **2008**, *130*, 15268−15269.
(25) Dietzel, P. D. C.; Georgiev, P. A.; Eckert, J.; Blom, R.; Strässle, T.; Unruh, T. Interaction of hydrogen with accessible metal sites in the metal−organic frameworks M_2(dhtp) (CPO-27-M; M = Ni, Co, Mg). *Chem. Commun.* **2010**, *46*, 4962−4964.
(26) FitzGerald, S. A.; Pierce, C. J.; Rowsell, J. L. C.; Bloch, E. D.; Mason, J. A. Highly selective quantum sieving of D_2 from H_2 by a metal−organic framework as determined by gas manometry and infrared spectroscopy. *J. Am. Chem. Soc.* **2013**, *135*, 9458−9464.
(27) FitzGerald, S. A.; Burkholder, B.; Friedman, M.; Hopkins, J. B.; Pierce, C. J.; Schloss, J. M.; Thompson, B.; Rowsell, J. L. C. Metal-specific interactions of H_2 adsorbed within isostructural metal-organic frameworks. *J. Am. Chem. Soc.* **2011**, *133*, 20310−20318.
(28) Kubas, G. J. Metal−dihydrogen and σ-bond coordination: the consummate extension of the Dewar−Chatt−Duncanson model for metal−olefin π bonding. *J. Organomet. Chem.* **2001**, *635*, 37−68.
(29) Caskey, S. R.; Wong-Foy, A. G.; Matzger, A. J. Dramatic tuning of carbon dioxide uptake via metal substitution in a coordination polymer with cylindrical pores. *J. Am. Chem. Soc.* **2008**, *130*, 10870−10871.
(30) Dietzel, P. D. C.; Besikiotis, V.; Blom, R. Application of metal−organic frameworks with coordinatively unsaturated metal sites in storage and separation of methane and carbon dioxide. *J. Mater. Chem.* **2009**, *19*, 7362−7370.
(31) Britt, D.; Furukawa, H.; Wang, B.; Glover, T. G.; Yaghi, O. M. Highly efficient separation of carbon dioxide by a metal-organic framework replete with open metal sites. *Proc. Natl. Acad. Sci. U.S.A.* **2009**, *106*, 20637−20640.
(32) Simmons, J. M.; Wu, H.; Zhou, W.; Yildirim, T. Carbon capture in metal−organic frameworks—a comparative study. *Energy Environ. Sci.* **2011**, *4*, 2177−2185.
(33) Yu, D.; Yazaydin, A. O.; Lane, J. R.; Dietzel, P. D. C.; Snurr, R. Q. A combined experimental and quantum chemical study of CO_2 adsorption in the metal-organic framework CPO-27 with different metals. *Chem. Sci.* **2013**, *4*, 3544−3556.
(34) Queen, W. L.; Hudson, M. R.; Bloch, E. D.; Mason, J. A.; Gonzalez, M. I.; Lee, J. S.; Gygi, D.; Howe, J. D.; Lee, K.; Darwish, T. A.; James, M.; Peterson, V. K.; Teat, S. J.; Smit, B.; Neaton, J. B.; Long, J. R.; Brown, C. M. Comprehensive study of carbon dioxide adsorption in the metal-organic frameworks M_2(dobdc) (M = Mg, Mn, Fe, Co, Ni, Cu, Zn). *Chem. Sci.* **2014**, *5*, 4569−4581.
(35) Dietzel, P. D. C.; Johnsen, R. E.; Fjellvåg, H.; Bordiga, S.; Groppo, E.; Chavan, S.; Blom, R. Adsorption properties and structure of CO_2 adsorbed on open coordination sites of metal−organic framework Ni_2(dhtp) from gas adsorption, IR spectroscopy and X-ray diffraction. *Chem. Commun.* **2008**, 5125−5127.
(36) Valenzano, L.; Civalleri, B.; Chavan, S.; Palomino, G. T.; Areán, C.; Bordiga, S. Computational and Experimental Studies on the Adsorption of CO, N_2, and CO_2 on Mg-MOF-74. *J. Phys. Chem. C* **2010**, *114*, 11185−11191.
(37) Poloni, R.; Smit, B.; Neaton, J. B. CO_2 capture by metal−organic frameworks with van der Waals density functionals. *J. Phys. Chem. A* **2012**, *116*, 4957−4964.
(38) Wu, H.; Simmons, J. M.; Srinivas, G.; Zhou, W.; Yildirim, T. Adsorption sites and binding nature of CO_2 in prototypical metal-organic frameworks: a combined neutron diffraction and first-principles study. *J. Phys. Chem. Lett.* **2010**, *1*, 1946−1951.
(39) Queen, W. L.; Brown, C. M.; Britt, D. K.; Zajdel, P.; Hudson, M. R.; Yaghi, O. M. Site-specific CO_2 adsorption and zero thermal expansion in an anisotropic pore network. *J. Phys. Chem. C* **2011**, *115*, 24915−24919.
(40) Kong, X.; Scott, E.; Ding, W.; Mason, J. A.; Long, J. R.; Reimer, J. A. CO_2 dynamics in a metal−organic framework with open metal sites. *J. Am. Chem. Soc.* **2012**, *134*, 14341−14344.
(41) Lin, L.-C.; Kim, J.; Kong, X.; Scott, E.; McDonald, T. M.; Long, J. R.; Reimer, J. A.; Smit, B. Understanding CO_2 dynamics in metal−organic frameworks with open metal sites. *Angew. Chem., Int. Ed.* **2013**, *52*, 4410−4413.

DOI: 10.1021/jp5104356
J. Phys. Chem. C 2015, 119, 5293−5300

(42) Kresse, G.; Hafner, J. Ab initio molecular dynamics for liquid metals. *Phys. Rev. B* **1993**, *47*, 558−561.
(43) Kresse, G.; Hafner, J. Ab initio molecular-dynamics simulation of the liquid-metal-amorphous-semiconductor transition in germanium. *Phys. Rev. B* **1994**, *49*, 14251−14269.
(44) Kresse, G.; Furthmüller, J. Efficiency of ab-initio total energy calculations for metals and semiconductors using a plane-wave basis set. *Comput. Mater. Sci.* **1996**, *6*, 15−50.
(45) Kresse, G.; Furthmüller, J. Efficient iterative schemes for ab initio total-energy calculations using a plane-wave basis set. *Phys. Rev. B* **1996**, *54*, 11169−11186.
(46) Liu, Y.; Kabbour, H.; Brown, C. M.; Neumann, D. A.; Ahn, C. C. Increasing the density of adsorbed hydrogen with coordinatively unsaturated metal centers in metal-organic frameworks. *Langmuir* **2008**, *24*, 4772−4777.
(47) Grimme, S. Semiempirical GGA-type density functional constructed with a long-range dispersion correction. *J. Comput. Chem.* **2006**, *27*, 1787−1799.
(48) Verma, P.; Xu, X. F.; Truhlar, D. G. Adsorption on Fe-MOF-74 for C1−C3 hydrocarbon separation. *J. Phys. Chem. C* **2013**, *117*, 12648−12660.
(49) Yu, K.; Kiesling, K.; Schmidt, J. R. Trace flue gas contaminants poison coordinatively unsaturated metal−organic frameworks: implications for CO_2 adsorption and separation. *J. Phys. Chem. C* **2012**, *116*, 20480−20488.
(50) Areán, C. O.; Chavan, S.; Cabello, C. P.; Garrone, E.; Palomino, G. T. Thermodynamics of hydrogen adsorption on metal-organic frameworks. *ChemPhysChem* **2010**, *11*, 3237−3242.
(51) Nijem, N.; Veyan, J. F.; Kong, L. Z.; Wu, H. H.; Zhao, Y. G.; Li, J.; Langreth, D. C.; Chabal, Y. J. Molecular hydrogen "pairing" interaction in a metal organic framework system with unsaturated metal centers (MOF-74). *J. Am. Chem. Soc.* **2010**, *132*, 14834−14848.
(52) Sumida, K.; Brown, C. M.; Herm, Z. R.; Chavan, S.; Bordiga, S.; Long, J. R. Hydrogen storage properties and neutron scattering studies of Mg_2(dobdc)—a metal−organic framework with open Mg^{2+} adsorption sites. *Chem. Commun.* **2011**, *47*, 1157−1159.
(53) Queen, W. L.; Bloch, E. D.; Brown, C. M.; Hudson, M. R.; Mason, J. A.; Murray, L. J.; Ramirez-Cuesta, A. J.; Peterson, V. K.; Long, J. R. Hydrogen adsorption in the metal−organic frameworks Fe_2(dobdc) and $Fe_2(O_2)$(dobdc). *Dalton Trans.* **2012**, *41*, 4180−4187.
(54) Brown, C. M.; Ramirez-Cuesta, A. J.; Her, J.-H.; Wheatley, P. S.; Morris, R. E. Structure and spectroscopy of hydrogen adsorbed in a nickel metal−organic framework. *Chem. Phys.* **2013**, *427*, 3−8.
(55) Bao, Z.; Yu, L.; Ren, Q.; Lu, X.; Deng, S. Adsorption of CO_2 and CH_4 on a magnesium-based metal organic framework. *J. Colloid Interface Sci.* **2011**, *353*, 549−556.
(56) Wilson, E. B., Jr.; Decius, J. C.; Cross, P. C. *Molecular Vibrations: The Theory of Infrared and Raman Vibrational Spectra*; Dover: New York, 1980.
(57) Calculations were performed using NBO 6.0: Glendening, E. D.; Badenhoop, J. K.; Reed, A. E.; Carpenter, J. E.; Bohmann, J. A.; Morales, C. M.; Landis, C. R.; Weinhold, F. *NBO 6.0*; Theoretical Chemistry Institute, University of Wisconsin, Madison, 2013.
(58) Poloni, R.; Lee, K.; Berger, R. F.; Smit, B.; Neaton, J. B. Understanding trends in CO_2 adsorption in metal−organic frameworks with open-metal sites. *J. Phys. Chem. Lett.* **2014**, *5*, 861−865.
(59) Lee, K.; Isley, W. C.; Dzubak, A. L.; Verma, P.; Stoneburner, S. J.; Lin, L.-C.; Howe, J. D.; Bloch, E. D.; Reed, D. A.; Hudson, M. R.; Brown, C. M.; Long, J. R.; Neaton, J. B.; Smit, B.; Cramer, C. J.; Truhlar, D. G.; Gagliardi, L. Design of a Metal-Organic Framework with Enhanced Back Bonding for Separation of N_2 and CH_4. *J. Am. Chem. Soc.* **2014**, *136*, 698−704.
(60) Rothman, L. S.; Gamache, R. R.; Goldman, A.; Brown, L. R.; Toth, R. A.; Pickett, H. M.; Poynter, R. L.; Flaud, J. M.; Camypeyret, C.; Barbe, A.; Husson, N.; Rinsland, C. P.; Smith, M. A. H. The HITRAN database: 1986 edition. *Appl. Opt.* **1987**, *26*, 4058−4097.
(61) Lopez, M. G.; Canepa, P.; Thonhauser, T. NMR study of small molecule adsorption in MOF-74-Mg. *J. Chem. Phys.* **2013**, *138*, 154704.

DOI: 10.1021/jp5104356
J. Phys. Chem. C 2015, 119, 5293−5300